HIGH RESOLUTION POLYNOMIAL UPWINDING SCHEMES FOR SOLVING 2D/3D FLUID DYNAMICS PROBLEMS

Giseli A B Lima, giabl@icmc.usp.br
Laís Corrêa, lacorrea@icmc.usp.br
Valdemir G Ferreira, pvgf@icmc.usp.br
Universidade de São Paulo, Avenida Trabalhor São-carlense, 400, CEP: 13560-970, São Carlos, São Paulo, Brasil

Abstract. *The correct modeling for processes involving convection, without introducing excessive artificial damping while retaining high accuracy, stability, boundedness and simplicity of implementation continues being nowadays a challenging task for the scientific CFD community. In this context, the objective of this study is to compare the performance of two new TVD-based upwinding schemes, namely, TOPUS and SDPUS-C1, with WENO scheme in the discretization of convective terms. These comparisons are done by the numerical results obtained for two/three-dimensional hyperbolic conservation laws, such as, 2D acoustics, 3D Burgers and 3D Euler equations. Finally, as application, the TOPUS and SDPUS-C1 schemes are used for the computational simulation of 3D incompressible fluid flows involving moving free surfaces.*

Keywords: *conservation laws, upwinding, high resolution, convection term*

1. INTRODUCTION

It is well known that in the process of numerical solution of PDEs which predominantly convective character the accuracy of the solutions is significantly affected by the choice of the convection scheme. For instance, first order upwind schemes, such as First Order Upwind (FOU) of Spalding (1972), are unconditionally stable, but they have a diffusive character that, in general, smoothed the solutions. On the order hand, classical high resolution schemes, such as central difference schemes, the Quadratic Upstream Interpolation for Convective Kinematics (QUICK) scheme (and its related QUICK with Estimated Stream Terms - QUICKEST) of Leonard (1988) can often produce unphysical oscillations which, most of the time, can lead to numerical instability. A very useful strategy that has been used nowadays is the non-linear upwinding discretization which adjusts themselves according to the local solution in order to maintain bounded behavior.

In this work, we present a two new polynomial upwinding schemes, namely: Third-Order Polynomial Upwind Scheme (TOPUS) of Queiroz (2010) and Six-Degree Polynomial Upwind Scheme of C^1 class (SDPUS-C1) of Lima (2010). These schemes were derived in the context of the Normalized Variable Diagram (NVD) of Leonard (1988), by enforcing the Total Variation Diminishing (TVD) constraint of Harten (1983). Consequently, they satisfy the Convection Boundedness Criterion (CBC) of Gaskell and Lau (1988).

The objective of this work is to compare the performance of these two new TVD-based upwinding schemes (TOPUS and SDPUS-C1) with the well established third/fifth-order WENO schemes (see Balsara and Shu (2000), Titarev and Toro (2004), Ketcheson and LeVeque (2006) and Zhang and Shu (2009)). The comparisons are done by using the numerical results obtained for two/three-dimensional hyperbolic conservation law systems. In the 2D case, we consider the linear acoustics equations. For the 3D case, we consider nonlinear conservation laws, such as Burgers and Euler equations. These conservation laws have been solved by mean of the Conservation LAW PACKage (CLAWPACK) of LeVeque *et al.* (2006) (equipped with TOPUS and SDPUS-C1 flux-limiter) and its extension called WENOCLAW of Ketcheson and LeVeque (2006).

Finally, as application, the TOPUS and SDPUS-C1 schemes are used for the computational simulation of three-dimensional incompressible fluid flows involving moving free surfaces. For these simulation, we have been used the 3D version of the Freeflow code of Castelo *et al.* (2000) equipped with both TOPUS and SDPUS-C1 schemes.

2. TOPUS AND SDPUS-C1 SCHEMES

Before proceeding to the derivation of the TOPUS and SDPUS-C1 schemes, it is essential to present the Normalized Variables (NV) of Leonard (1988) and the conditions required for the construction of a monotonic upwinding scheme (see Leonard (1988) and Lin and Cheing (1991)) (using the TVD and CBC criteria).

In order to interpolate the numerical flux ϕ_f at a boundary face f between two control volumes, we will use, in one-dimensional case, three neighboring grid points, namely Downstream (D), Upstream (U) and Remote-upstream (R), and the convecting velocity, V_f, at this face (see Fig. 1). For multidimensional problems, this strategy is applied in the same fashion, with each convective derivative approximated along of the relevant variable (direction-by-direction). So, the scheme is given by the function

$$\phi_f = \phi_f(\phi_D, \phi_U, \phi_R). \tag{1}$$

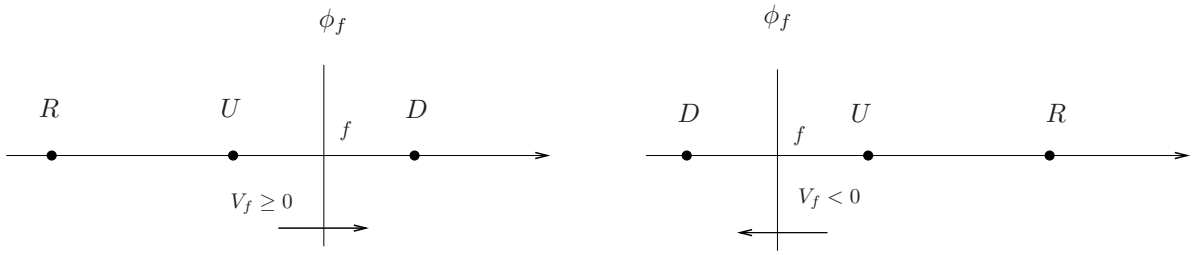

Figure 1. Interfaces and their related grid points for determining an upwinding scheme.

To simplify the functional relationship given by Eq. (1) the original variables are transformed in NV as

$$\hat{\phi}_{[\ ]} = \frac{\phi_{[\ ]} - \phi_R}{\phi_D - \phi_R}. \tag{2}$$

The advantage of this new formulation is that the value $\hat{\phi}_f$ depends on $\hat{\phi}_U$ only, since $\hat{\phi}_D = 1$ and $\hat{\phi}_R = 0$. Thus, Eq. (1) can be rewritten as

$$\hat{\phi}_f = \hat{\phi}_f(\hat{\phi}_U). \tag{3}$$

According to Leonard (1988), for $0 \leq \hat{\phi}_U \leq 1$, it is possible to derive a non-linear monotonic third-order NV scheme imposing the following conditions on Eq. (3), namely: $\hat{\phi}_f(1) = 1$; $\hat{\phi}_f(0) = 0$; $\hat{\phi}_f(1/2) = 3/4$; and $\hat{\phi}_f^{'}(1/2) = 3/4$. Leonard (1988) also recommends that for values of $\hat{\phi}_U \leq 0$ or $\hat{\phi}_U \geq 1$, the scheme must be extended in a continuous manner using the FOU scheme, which is defined by

$$\hat{\phi}_f = \hat{\phi}_U. \tag{4}$$

In this context, Gaskell and Lau (1988) (see also Waterson and Deconinck (2007)) proposed the CBC criterion, which is a necessary and sufficient condition for a scheme possessing boundedness, namely:

$$\begin{cases} \hat{\phi}_U \leq \hat{\phi}_f(\hat{\phi}_U) \leq 1 & \text{if} \quad \forall \hat{\phi}_U \in [0,\ 1] \\ \hat{\phi}_f = \hat{\phi}_f(\hat{\phi}_U) = \hat{\phi}_U & \text{if} \quad \forall \hat{\phi}_U \notin [0,\ 1] \\ \hat{\phi}_f(\hat{\phi}_U) = 1 & \text{and} \quad \hat{\phi}_f(0) = 0. \end{cases} \tag{5}$$

These conditions determine the CBC region (see Fig. 2).

Another important convective stability criterion is the TVD constraint of Harten (1983), which ensures that spurious oscillations are removed from the numerical solution. In summary, considering a sequence of discrete approximations $\phi(t) = \phi_i(t)$ to a scalar, where i is an integer, the total variation (TV) at time t of this sequence is defined by

$$TV(\phi(t)) = \sum_i |\phi_{i+1}(t) - \phi_i(t)|. \tag{6}$$

Then, the scheme is TVD if the following conditions is satisfied

$$TV(\phi^{n+1}) \leq TV(\phi^n), \quad \forall n. \tag{7}$$

In addition, the TVD concept was translated by Sweby (1984) into a set of limitations for the behavior of a functional relationship given by Eq. (3), namely

$$\begin{cases} \hat{\phi}_f \in [\hat{\phi}_U, 2\hat{\phi}_U] \text{ and } \hat{\phi}_f \leq 1, & \text{if} \quad \hat{\phi}_U \in [0,1], \\ \hat{\phi}_f = \hat{\phi}_U, & \text{if} \quad \hat{\phi}_U \notin [0,1], \end{cases} \tag{8}$$

which led the TVD region for $\hat{\phi}_f(\hat{\phi}_U)$ (see Fig. 2).

After one to have developed a NVD/TVD-based upwind scheme, we derive the associated flux-limiter by rewriting the original scheme in the following way (see Sweby (1984) and Waterson and Deconinck (2007)):

$$\hat{\phi}_f = \hat{\phi}_U + \frac{1}{2}\psi(r)(1 - \hat{\phi}_U), \tag{9}$$

where $\psi(r)$ is the flux-limiter that determines the level of antidifusividade and r being a local shock sensor given by ratio of consecutive gradients. In uniform meshes and in NV, r is given by

$$r = \frac{\hat{\phi}_U}{1 - \hat{\phi}_U}. \tag{10}$$

In addition, the TVD concept was also translated by Sweby (1984) into a set of limitations for dictating the behavior of the flux-limiter function, given by

$$\begin{cases} \psi(r) = 0, & \text{if} \quad r \leq 0, \\ 0 \leq \psi(r) \leq \min\{2, 2r\}, & \text{if} \quad r > 0. \end{cases} \tag{11}$$

Theses conditions define the TVD region for $\psi(r)$ (see Fig. 2).

In summary, Fig. 2 shows geometrically the regions for the three stability criteria discussed before.

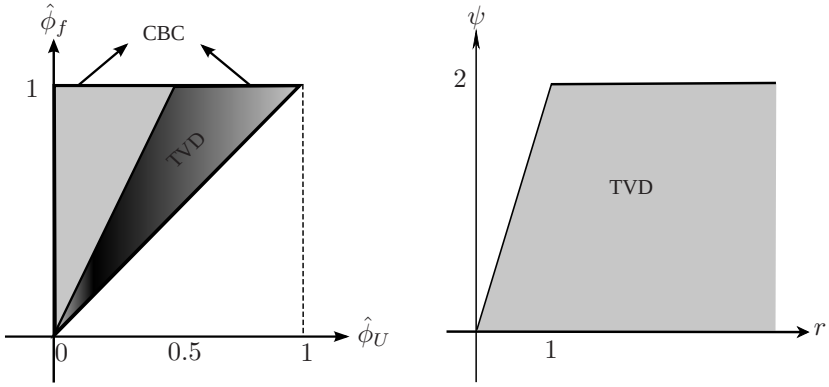

Figure 2. Stability criteria: the CBC and TVD regions for $\hat{\phi}_f(\hat{\phi}_U)$ (left) and the TVD region for $\psi(r)$ (right).

2.1 Development of TOPUS and SDPUS-C1 schemes

In particular, the TOPUS and SDPUS-C1 schemes were derived in the context of NV of Leonard (1988) and TVD constraint of Harten (1983). The numerical solutions obtained by these schemes can be second or third order accurate in the smooth parts of the solution, but first order near regions with large gradients. The TOPUS scheme of Queiroz (2010) was derived by assuming that the NV at the cell interface f, $\hat{\phi}_f$, is related to $\hat{\phi}_U$ as a four-degree polynomial function of the form $\hat{\phi}_f = \sum_{k=0}^{4} a_k \hat{\phi}_U^k$, for $0 \leq \hat{\phi}_U \leq 1$, and a linear function (the FOU scheme) given by Eq. (4), for $\hat{\phi}_U < 0$ or $\hat{\phi}_U > 1$. A free parameter (say $a_4 = \alpha$) is considered and the other coefficients are determined by imposing the four conditions of Leonard (1988) outlined above. The SDPUS-C1 scheme of Lima (2010) is derived in the same way as TOPUS scheme. For this case, it is considered a six-degree polynomial function of the form $\hat{\phi}_f = \sum_{k=0}^{6} b_k \hat{\phi}_U^k$, for $0 \leq \hat{\phi}_U \leq 1$, and the FOU scheme (Eq. (4)), for $\hat{\phi}_U < 0$ or $\hat{\phi}_U > 1$. We set a free parameter (say $b_2 = \gamma$) and determine the other coefficients by imposing the four conditions of Leonard outlined above, plus the conditions of continuous differentiability for $\hat{\phi}_f = \hat{\phi}_f(\hat{\phi}_U)$ on the whole remains. In other works the six-degree polynomial function and Eq. (4) are linked on the points $(0, 0)$ and $(1, 1)$ with the same values for the first derivatives. Thus, the SDUPS-C1 scheme is a continuously differentiable function. It is important to note here that, according to Lin and Chieng (1991), if this property is not satisfied then convergence problems may be found in unsteady calculations when large time steps are employed. In summary, the schemes are:

– TOPUS:

$$\hat{\phi}_f = \begin{cases} \alpha\hat{\phi}_U^4 + (1-2\alpha)\hat{\phi}_U^3 + \frac{(-10+5\alpha)}{4}\hat{\phi}_U^2 + \frac{(10-\alpha)}{4}\hat{\phi}_U & \hat{\phi}_U \in [0,1], \\ \hat{\phi}_U, & \hat{\phi}_U \notin [0,1], \end{cases} \tag{12}$$

where α is a free parameter.

– SDPUS-C1:

$$\hat{\phi}_f = \begin{cases} (-24+4\gamma)\hat{\phi}_U^6 + (68-12\gamma)\hat{\phi}_U^5 + (-64+13\gamma)\hat{\phi}_U^4 + (20-6\gamma)\hat{\phi}_U^3 + \gamma\hat{\phi}_U^2 + \hat{\phi}_U, & \hat{\phi}_U \in [0,1], \\ \hat{\phi}_U, & \hat{\phi}_U \notin [0,1], \end{cases} \tag{13}$$

where γ is a free parameter.

The corresponding flux-limiter functions for the TOPUS and SDPUS-C1 schemes are derived by combining, respectively, Eq. (12) and Eq. (13), with Eq. (9) and Eq. (10) to obtain,

$$\psi(r) = \max\left\{0, \ \frac{0.5(|r|+r)[(1-0.5\alpha)r^2 + (4+\alpha)r + (3-0.5\alpha)]}{(1+|r|)^3}\right\} \tag{14}$$

and

$$\psi(r) = \max\left\{0, \ \frac{0.5(|r|+r)[(-8+2\gamma)r^3 + (40-4\gamma)r^2 + 2\gamma r]}{(1+|r|)^5}\right\}. \tag{15}$$

It is possible by mean of numerical tests to show that the TOPUS scheme is TVD for $\alpha \in [0, 2]$ (see Queiroz (2010)) and SDPUS-C1 scheme for $\gamma \in [4, 12]$ (see Lima (2010)). In this work, we considered $\alpha = 2$ and $\gamma = 12$. For these values Queiroz (2010) and Lima (2010) have shown that both the TOPUS and SDPUS-C1 schemes have presented good results for problems with discontinuities. In Fig. 3 are depicted the TOPUS (for $\alpha = 2$) and SDPUS-C1 (for $\gamma = 12$) scheme (left) and the their flux-limiters (right).

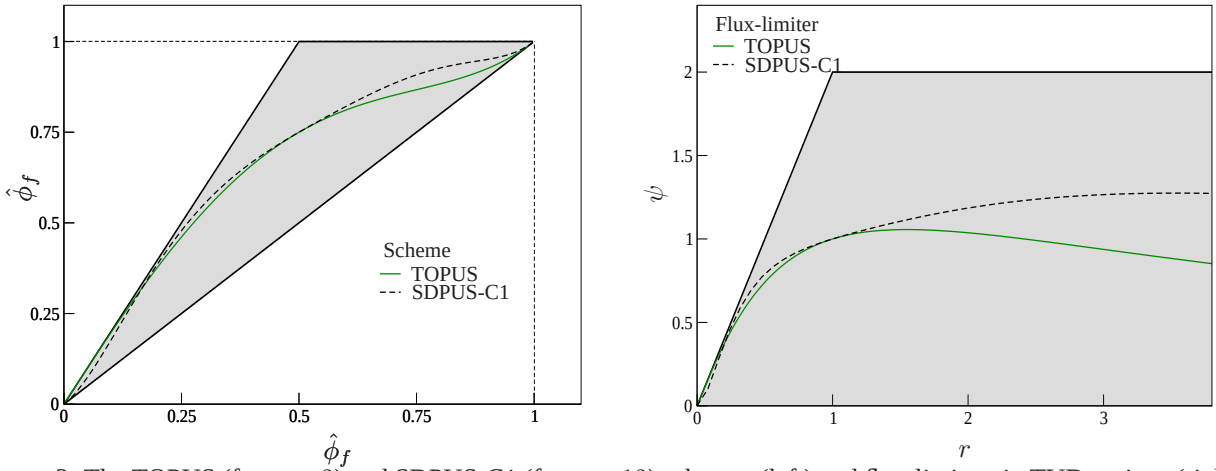

Figure 3. The TOPUS (for $\alpha = 2$) and SDPUS-C1 (for $\gamma = 12$) schemes (left) and flux-limiters in TVD regions (right).

3. NUMERICAL RESULTS

We now discuss the performance of the TOPUS and SDPUS-C1 schemes and compare their results with those of WENO schemes. For this we used the 2D/3D hyperbolic conservation laws. Then, as application, the TOPUS and SDPUS-C1 schemes are used for simulating the 3D circular hydraulic jump.

3.1 Conservation laws

Many problems in science and engineering involve quantities that are preserved and that lead to certain types of PDEs called hyperbolic conservation laws. These laws are generally nonlinear and time-dependent. In the three-dimensional case, they are defined by

$$\frac{\partial \phi}{\partial t} + \frac{\partial F(\phi)}{\partial x} + \frac{\partial G(\phi)}{\partial y} + \frac{\partial H(\phi)}{\partial z} = 0, \tag{16}$$

where $\phi = \phi(x, y, z, t)$ is the vector of the conservation variables and $F(\phi) = F(\phi(x, y, z, t))$, $G(\phi) = G(\phi(x, y, z, t))$ and $H(\phi) = G(\phi(x, y, z, t))$ are flux functions. In the two-dimensional case of these laws the $H(\phi) = H(\phi(x, y, t))$ is neglected, the ϕ, $F(\phi)$ and $G(\phi)$ respectively are given by $\phi = \phi(x, y, t)$, $F(\phi) = F(\phi(x, y, t))$ and $G(\phi) = G(\phi(x, y, t))$. Here we consider three particular cases of these laws, namely: 2D acoustics, 3D Burgers and 3D Euler equations. In order to resolve these equations, the well established CLAWPACK of LeVeque (2004) and its extension, namely WENOCLAW of Ketcheson and LeVeque (2006), have been used. These softwares packages and additional documentations are freely available in LeVeque *et al.* (2006). The method implemented in CLAWPACK employs the finite volume methodology and a wave propagation approach (LeVeque, 2004). In this work, we combine this method with the TOPUS and SDPUS-C1 flux-limiter given by Eq. (14) and Eq. (15), respectively. The method employed in WENOCLAW combines the notions of wave propagation and line methods (Ketcheson and LeVeque, 2006) . The WENOCLAW is implemented based on CLAWPACK and makes use of Riemann solvers in the same form required for this softwares package (Ketcheson and LeVeque, 2006). The numerical solutions from both codes, CLAWPACK and WENOCLAW, are dimensionless (see LeVeque (2004) and Ketcheson and LeVeque (2006) for more details).

3.1.1 2D acoustics equations

The acoustics equations are formulated by Eq. (16), with the vector of the conservation variables given by $\phi = [p, u, v]^T$ and flux functions by $F(\phi) = [Ku, p/\rho, 0]^T$ and $G(\phi) = [Kv, 0, p/\rho]^T$. Here $[u, v]^T$ is the velocity vector, and K, ρ and p are bulk modulus of compressibility of the material, density and pressure, respectively (for details, the reader is referred to LeVeque (2004)). This system is solved in the domain $[0, 1] \times [0, 1]$, where the interface line $x = 0.5$ separates two materials (one on the left and another on the right) with density ρ and sound speed c given by $\rho_L = 1$, $c_L = 1$, and

$\rho_R = 4$, $c_R = 0.5$. Another datum for the simulation is the pulse for the pressure which leads to a radially-symmetric disturbance, namely

$$r = \sqrt{(x-0.25)^2 + (y-0.4)^2}. \tag{17}$$

The initial conditions are

$$u(x,y,0) = v(x,y,0) = 0, \quad p(x,y,0) = \begin{cases} 1 + 0.5\left[\cos\left(\frac{\pi \cdot r}{0.1}\right) - 1\right], & \text{if} \quad r < 0.1, \\ 0, & \text{otherwise.} \end{cases} \tag{18}$$

Zero-order extrapolation is considered on the boundary.

For the simulation of this problem, we calculated the reference solution by using the CLAWPACK code, where the Godunov method with the correction term (containing the Monotonized central-difference (MC) flux-limiter) is used. For this, we consider 400×400 computational cells and the Courant number $\theta = 0.45$ (see LeVeque et al. (2006)). The numerical solutions are obtained with the same Godunov method, but using the TOPUS and SDPUS-C1 flux-limiters. For these solutions, a mesh size of 100×100 computational cells, $\theta = 0.45$ and $\theta = 0.9$ are used. The results for WENO scheme are obtained by using WENOCLAW code in the same mesh (100×100 computational cells) and Courant numbers ($\theta = 0.45$ and $\theta = 0.9$).

In Fig. 4 and Fig. 5, we presented at final time of simulation $t = 0.5$ the pressure variation as a function of distance from the origin (ie, p on line $y = 0$). In these figures we compared the TOPUS, SDPUS-C1 and WENO schemes with the MC reference solution. It is possible to see that in the case of $\theta = 0.45$ the WENO scheme provides better results than those obtained with TOPUS and SDPUS-C1 schemes (see Fig. 4). This occurs principally in the capture of the peak and valley in the range $x \in [0.5,\ 0.7]$. On the order hand, in the case of $\theta = 0.9$, the TOPUS and SDPUS-C1 schemes provide the best results in the domain (see Fig. 5).

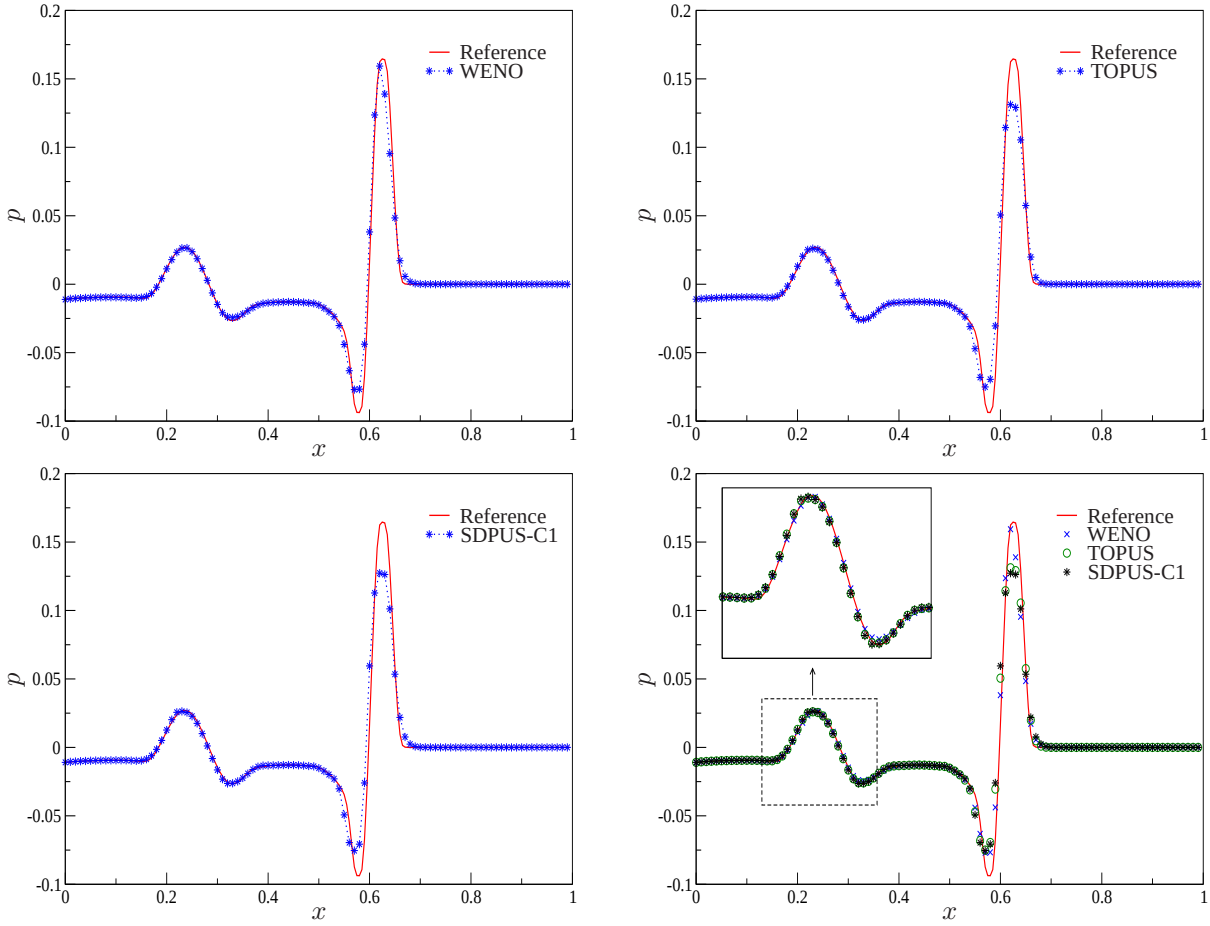

Figure 4. Solutions for 2D acoustics equations obtained with WENO, TOPUS and SDPUS-C1 schemes, for p on line $y = 0$, at $t = 0.5$ and $\theta = 0.45$.

Figure 6 shows the results of the SDPUS-C1 scheme for cross-section from the simulation of the pressure at $t = 0$, $t = 0.5$ and $t = 1$. The other results obtained with the TOPUS and WENO schemes are omitted due to their similarities. One can also observe from this figure that when the pressure pulse hits the interface, it is partially reflected and partially transmitted.

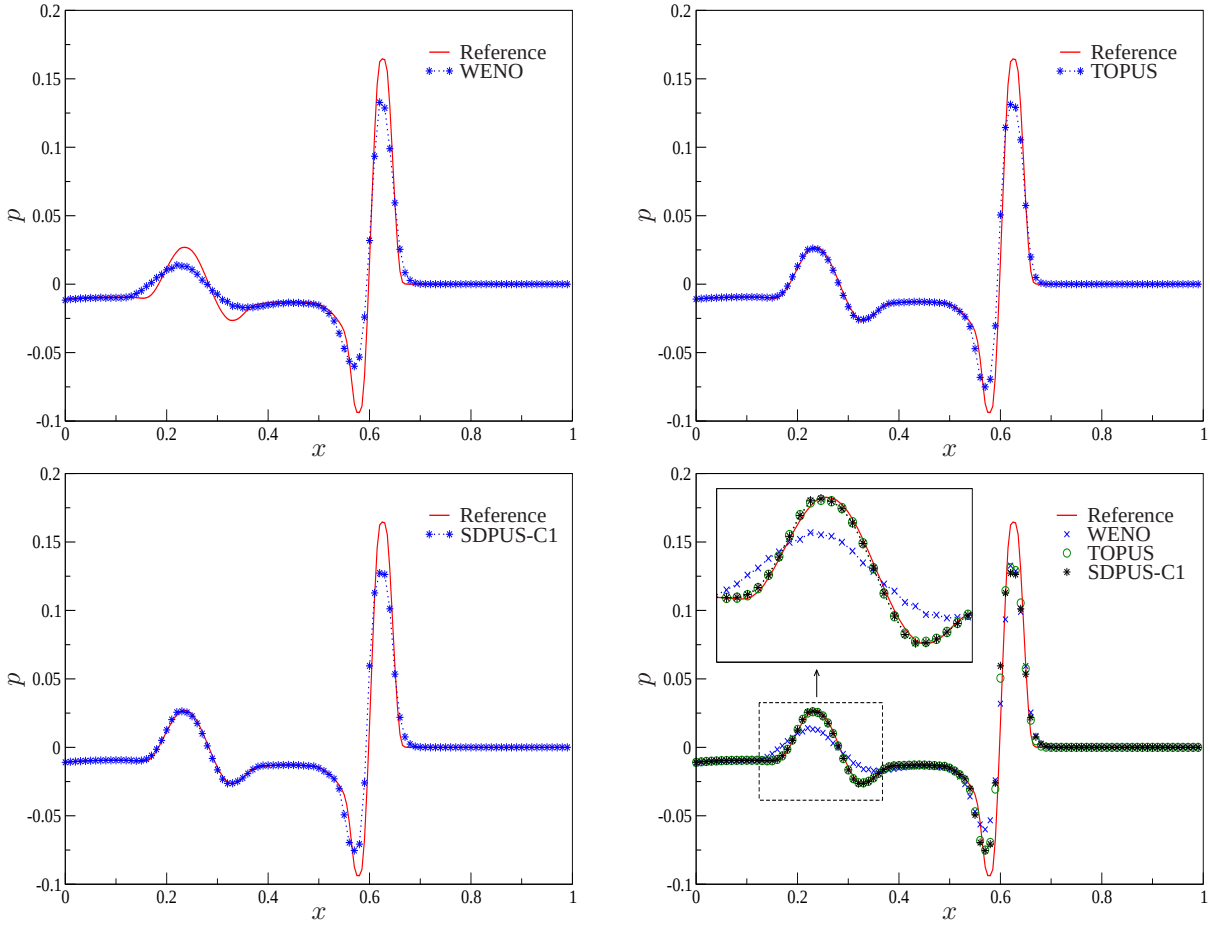

Figure 5. Solutions for 2D acoustics equations obtained with WENO, TOPUS and SDPUS-C1 schemes, for p on line $y = 0$, at $t = 0.5$ and $\theta = 0.9$.

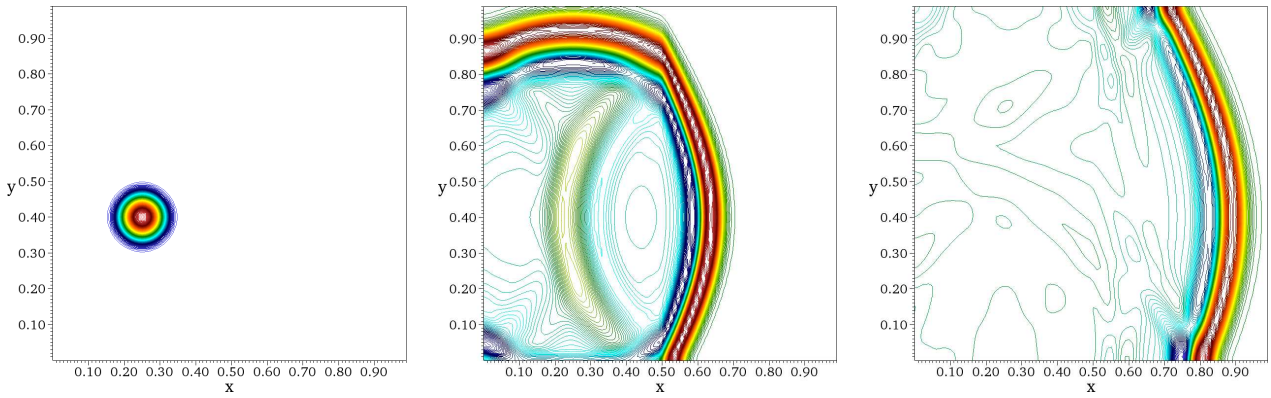

Figure 6. Solutions for 2D acoustics equations obtained by SDPUS-C1 scheme for cross-section of the p at $t = 0$, $t = 0.5$ and $t = 1$.

3.1.2 3D Burgers equation

The 3D Burgers equations correspond to Eq. (16) with the vector of the conservation variables given by $\phi = u$ and flux functions $F(\phi) = G(\phi) = H(\phi) = \frac{1}{2}u^2$. Here u is the velocity vector. These equations are defined in $[-3, 3] \times [-3, 3] \times [-3, 3]$, supplemented with the initial data

$$u(x, y, z, 0) = 0.3 + 0.7\sin\left(\frac{\pi}{3}(x + y + z)\right) \tag{19}$$

and periodic boundary conditions.

This hyperbolic system is solved by using CLAWPACK code. The reference solution is obtained on a mesh size of $100 \times 100 \times 100$ computational volumes by using the Godunov method with the correction term employing the MC

flux-limiter (see LeVeque (2004)). The numerical solutions are calculated by using of the TOPUS and SDPUS-C1 flux-limiters, on a uniform mesh of $50 \times 50 \times 50$ finite volumes. For both cases (numerical and reference), we considered $\theta = 0.27$. The result for WENO scheme was obtained from the article of the Zhang and Shu (2009).

In Fig. 7 it is depicted the reference and numerical solutions for the u component at $t = \frac{5}{\pi^2}$, on line $x = y$ and $z = 0$. We can observe, from this figure, that the solutions with TOPUS, SDPUS-C1 and WENO schemes are similar, presenting non-oscillatory results and capturing very well the shock. However, the WENO scheme presents two solution-points on shocks, while both the TOPUS and SDPUS-C1 show only one. In Fig. 8, it is depicted the result obtained with the TOPUS scheme for u velocity in $x \perp y$ (left) and $x \perp y \perp z$ (right). The results with the SDPUS-C1 and WENO scheme are omitted due their similarities with the result with TOPUS scheme. We can see for this figure that the results are in good agreement with the solutions of Zhang and Shu (2009).

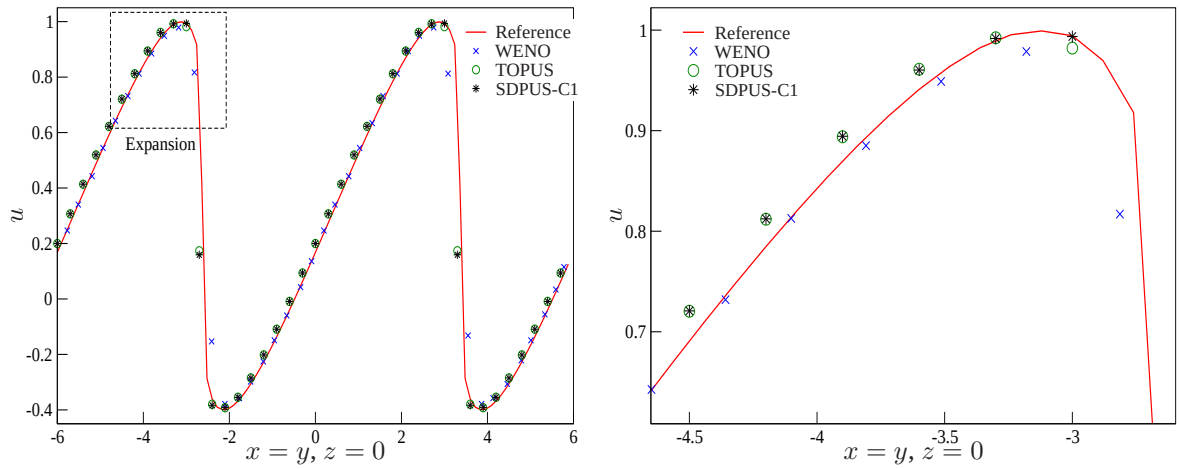

Figure 7. Solutions for the 3D Burgers equations obtained by using the WENO, TOPUS and SDPUS-C1 schemes(left) and a expansion of the results (right), for u, on line n $x = y$ and $z = 0$, at $t = \frac{5}{\pi^2}$.

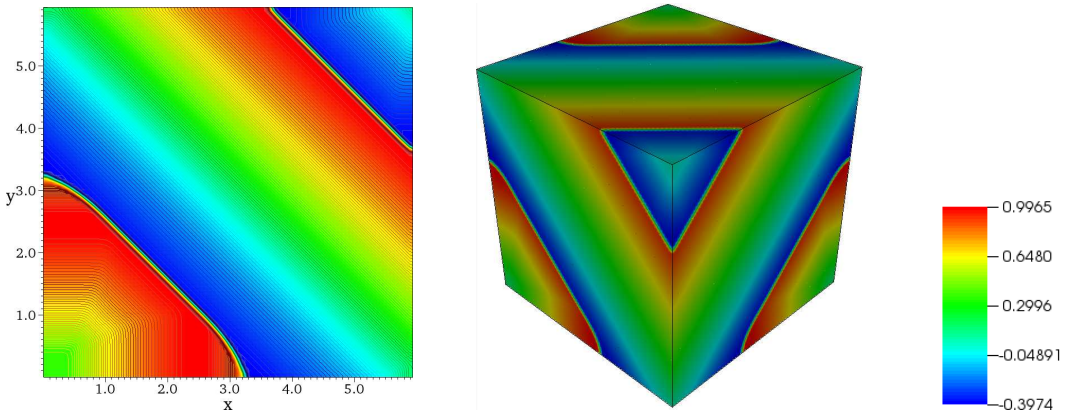

Figure 8. Solutions for the 3D Burgers equations obtained by the TOPUS scheme for u, on line n $x \perp y$ (left) and $x \perp y \perp z = 0$ (right) at $t = \frac{5}{\pi^2}$.

3.1.3 3D Euler equations

The Euler equations are given by Eq. (16), where $\phi = [\rho, \rho u, \rho v, \rho w, E]^T$ is the vector of conserved quantities, $F(\phi) = [\rho u, \rho u^2 + p, \rho uv, \rho uw, (E+p)u]^T$, $G(\phi) = [\rho v, \rho uv, \rho v^2 + p, \rho vw, (E+p)v]^T$ and $H(\phi) = [\rho w, \rho uw, \rho vw, \rho w^2 + p, (E+p)w]^T$ are flux functions; being ρ, u, v, w, ρu, ρv, ρw, E and p the density, the x-velocity, the y-velocity, the w-velocity, the x-momentum, the y-momentum, the w-momentum, the total energy and the pressure, respectively. In order to close the system, the ideal gas equation of state $p = (\lambda - 1)(E - \frac{1}{2}\rho(u^2 + v^2 + w^2))$ with $\lambda = 1.4$ is considered.

We consider the so-called spherical explosion test as a representative problem for 3D Euler equations (see Titarev and Toro (2004)). The problem consists of two regions, separated by a sphere of radius 0.4, with values for gas parameters differents. The problem is solved in the domain $[-1, 1] \times [-1, 1] \times [-1, 1]$, and the Euler equations are supplemented

with the initial conditions

$$(\rho(x,y,z,0),p(x,y,z,0))^T = \begin{cases} (1.0,\ \ 1.0)^T & \text{if} \quad r \leq 0.4 \\ (0.125,\ \ 0.1)^T & \text{if} \quad r > 0.4, \end{cases} \tag{20}$$

where $u = v = w = 0$, $r^2 = x^2 + y^2 + z^2$. Zero-order extrapolation on the boundary is assumed.

The reference solution is obtained by applying the strategy proposed by Toro (1999) in the 1D version of the CLAWPACK code. The first-order Godunov method on 1000 computational cells and $\theta = 0.27$ have been used. The numerical solutions are calculated via 3D version of CLAWPACK, using the Godunov method with the correction term containing the TOPUS and SDPUS-C1 flux-limiters. A mesh size of $100\times100\times100$ computational cells and $\theta = 0.27$ are employed. The results with WENO scheme were obtained from Titarev and Toro (2004). Figure 9 depicts the solutions (reference and numerical) for the density along the x axis ($y = z = 0$) at time $t = 0.25$. It can clearly see from this figure that the results with TOPUS, SDPUS-C1 and WENO schemes are similar. As an illustration, we present in Fig. 10 the results obtained with the SDPUS-C1 scheme for ρ in $x \perp y$, at $t = 0$, $t = 0.25$ and $t = 0.5$ with $\theta = 0.27$. The results obtained with TOPUS and WENO schemes are not presented due to similarity to the results generated by the SDPUS-C1 scheme.

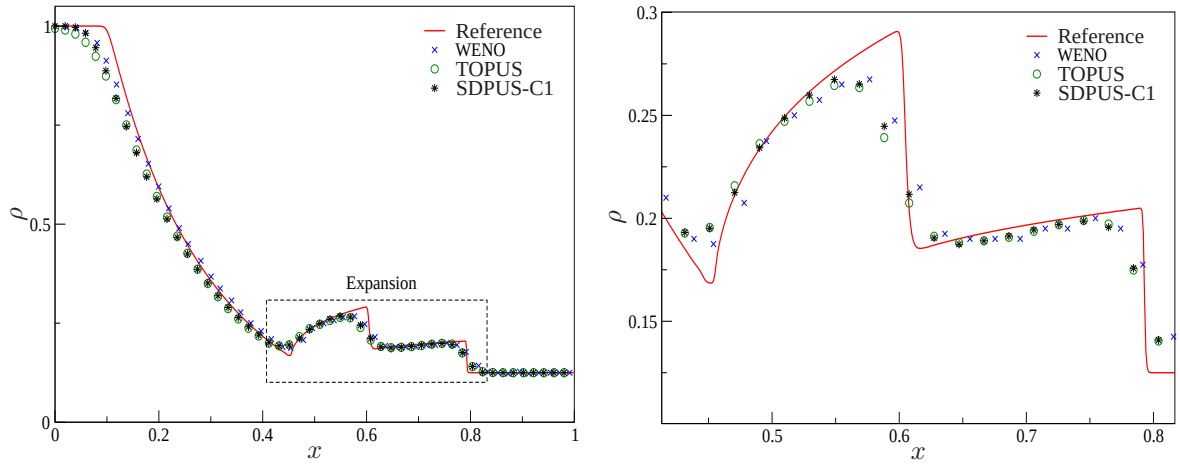

Figure 9. Solutions for the 3D Euler equations obtained by the WENO, TOPUS and SDPUS-C1 schemes (left) and expansion of results (right) for ρ in x axis at $t = 0.25$ and $\theta = 0.27$.

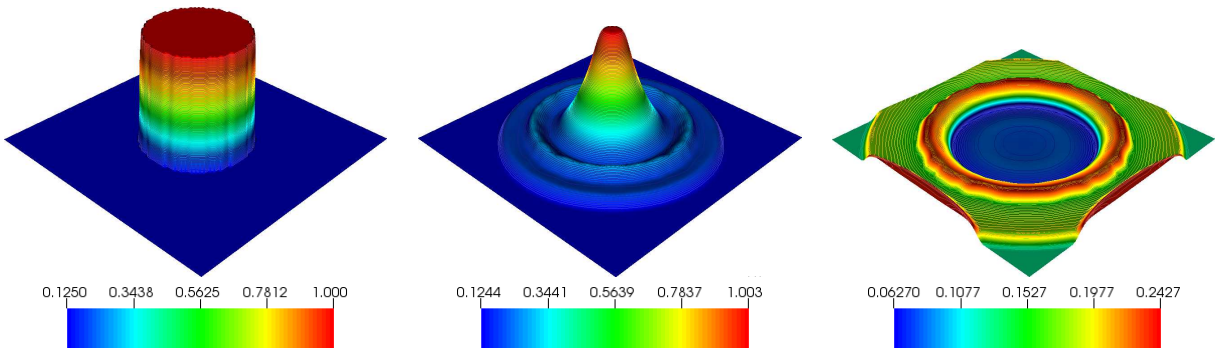

Figure 10. Results generated by SDPUS-C1 scheme for ρ in $x \perp y$ at $t = 0$, $t = 0.25$ and $t = 0.5$ with $\theta = 0.27$.

3.2 Navier-Stokes equations

From now on, we examine the capability of the TOPUS and SDPUS-C1 schemes for solving complex 3D flow problems involving moving free surfaces. For this, we considered a vertical free jet impinging perpendiculary onto an impermeable rigid surface (under the gravitational field), leading to the formation of a curious phenomenon, observable in everyday life, known as circular hydraulic jump (see reference Ellegaard et al. (1996) for more details on the phenomenon). For the simulation of this free surface flow, we have used the 3D version Freeflow code of Castelo *et al.* (2000) equipped with both TOPUS and SDPUS-C1 schemes. The governing equations are Navier-Stokes and mass conservation equations and they are given, respectively, by

$$\frac{\partial \mathbf{u}}{\partial t} + \nabla \cdot (\mathbf{uu}) = -\nabla p + \nu \nabla^2 \mathbf{u} + g, \tag{21}$$

$$\nabla \cdot \mathbf{u} = 0, \tag{22}$$

where $\mathbf{u} = [u(x,y,z,t),\ v(x,y,z,t)\, w(x,y,z,t)]^T$ is the velocity vector field, p is the pressure, g gravitational field and ν is the viscosity coefficient (constant).

The circular hydraulic jump may arise when a free jet of water falling vertically at moderate Reynolds number strikes a horizontal rigid surface. A better understanding of the phenomenon and the instabilities, at least in its turbulent form, is of commercial interest, since jet impingement is often used in cooling systems and the flow of the fluid beyond the jump can degrade the efficiency of the system. Therefore, a 3D turbulent hydraulic jump constitutes an excellent test for validating codes based on front tracking techniques. In order to solve this phenomenon, we consider a domain of $0.6\,m \times 0.6\,m \times 0.6\,m$, where the diameter and height (from inlet to the rigid surface) of inlet are given by $D = 0.05\,m$ and $H = 0.001\,m$, respectively. In addition, we employed the following data: the velocity scale $u_0 = u_{max} = 1.0\,m/s$ (injection speed); length scale $D = 0.05$; coefficient of kinematic viscosity $\nu = 5 \times 10^{-5}\,m/s$ and gravitational constant $g = 9.81\,m/s^2$. The Reynolds number is based on the injection speed and diameter of the inlet, namely, $Re = \frac{u_0\, D}{\nu} = 1000$.

Figure 11 shows a qualitative comparison between the experimental results of Ellegaard *et al.* (1996) and the results obtained with TOPUS and SDPUS-C1 schemes. One can clearly see from this figure that our numerical method equipped with these high resolution polynomial upwind schemes captured the complete physical mechanism of this complex free surface flow.

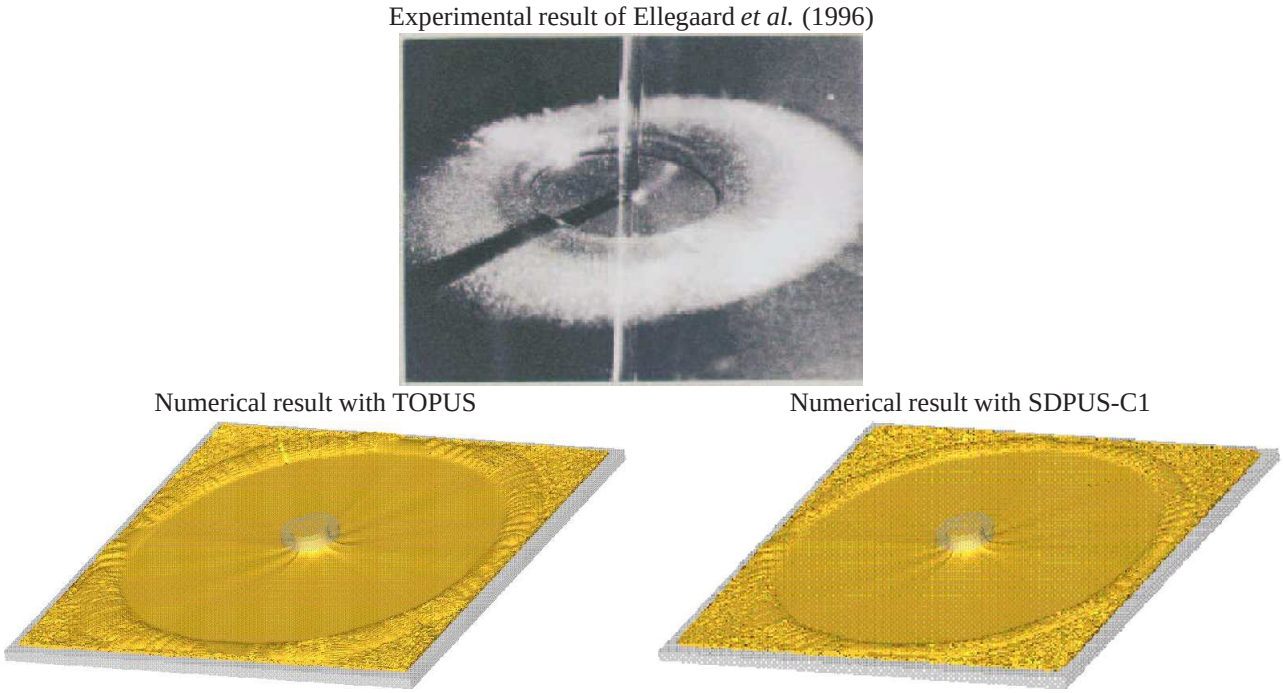

Figure 11. 3D qualitative comparison between the experimental and numerical results for a turbulent hydraulic jump using TOPUS and SDPUS-C1 schemes.

4. CONCLUSIONS

In this paper, two high resolution polynomial upwinding schemes (TOPUS and SDPUS-C1) were compared with WENO schemes (Balsara and Shu (2000), Titarev and Toro (2004), Ketcheson and LeVeque (2006) and Zhang and Shu (2009)). By using these schemes, various test problems formulated by two/three-dimensional conservation laws, such as, 2D acoustics, 3D Burgers and 3D Euler equations were solved. With these results, we may conclude that both the polynomial schemes provide similar results to those generated by WENO schemes (which is well established class of schemes in the literature). It can be observed in the literature (see the papers in the reference section) that the WENO schemes are, from computational point of view, more expensive than the TOPUS (Queiroz, 2010) and SDPUS-C1 (Lima, 2010) schemes. So, we have in hand two new upwinding schemes which are computationally simpler than the WENO schemes and provide us similar results to the WENO schemes. As an application, the TOPUS and SDPUS-C1 schemes were used to simulate three-dimensional incompressible flows involving free surfaces. Once more, the results demonstrated that these upwinding schemes are effective tools for studying complex fluid dynamics problems. For the future, the authors are planning to apply SDPUS-C1 scheme to the numerical solution of three-dimensional turbulent

viscoelastic free surface flows.

5. ACKNOWLEDGEMENTS

We thank the financial support given by FAPESP (Grants 2008/07367-9 and 2009/16954-8) and CNPq (Grants 300479/2008-5). This work was also carried onto in the framework of the Instituto Nacional de Ciência e Tecnologia em Medicina Assistida por Computação Científica (CNPq Brazil).

6. REFERENCES

Balsara, D.S. and Shu, C.W., 2000. "Monotocicity preserving weighted essentially non-oscillatory scheme with increasingly high order of accuracy". *Journal of Computational Physics*, Vol. 160, pp. 405-452.

Castelo, A., Tomé, M.F., McKee, S., Cuminato, J.A. and Cesar, C.N.L., 2000. "Freeflow: an integrated simulation system for three-dimensional free surface flows". *Computing and Visualization in Science*, Vol. 2, pp. 1-12.

Ellegaard, C., Hansen, A.E., Haaning, A. and Bohr, T., 1996. "Experimental results on flow separation and transitions in the circular hydraulic jump". *Physica Scripta*, Vol. 67, pp. 105-110.

Gaskell, P.H. and Lau, K.C., 1988. "Curvature-compensated convective transport: Smart, a new boundedness preserving transport algorithm". *International Journal of Numerical Methods in Fluids*, Vol. 8, pp. 617-641.

Harten, A., 1983. "High resolution schemes for hyperbolic conservation laws". *Journal of Computational Physics*, Vol. 49, pp. 357-393.

Ketcheson, D.I. and LeVeque, R.J., 2006. "WENOCLAW: a higher order wave propagation method", *In Proceedings of the 11th International Conference on Hyperbolic Problems*. Lyon, France.

Leonard, B.P., 1988. "Simple high-accuracy resolution program for convective modeling of discontinuities". *International Journal for Numerical Methods in Fluids*, Vol. 8, pp. 1291-1318.

LeVeque R.J., Langseth, J.O., Berger, M., McQuenn, D., Calhoun, D., Blossy, P. and Mitran, S., 2006. "Conservation Law Package (CLAWPACK) Version 4.3-User's guide". 10 Mar. 2011 <http://www.amath.washington.edu/∼claw/>.

LeVeque, R.J., 2004. *Finite volumes methods for hyperbolic problems.* Cambridge University Press, New York, U.S.A.

Lima, G.A.B., 2010. *Desenvolvimento de estratégias de captura de descontinuidades para leis de conservação e problemas relacionados em dinâmica dos fluidos*. Masters thesis, Universidade de São Paulo, São Carlos, Brazil.

Lin, H. and Chieng, C.C., 1991. "Characteristic-based flux limiters of an essentially third-order flux-splitting method for hyperbolic conservation laws". *International Journal for Numerical Methods in Fluids*, Vol. 13, pp. 287-307.

Queiroz, R.A.B. and Ferreira, V.G., 2010. *Development and testing of high-resolution upwind schemes- upwind schemes for incompressible free surface flows*. VDM Verlag Dr. Muler Aktiengesellschaft & Co. KG and Licensors, U.S.A.

Spalding, D.B., 1972. "Anovel finite difference formulation for differential expressions involving both first and second derivatives". *International Journal for Numerical Methods in Fluids*, Vol. 4, pp. 551-559.

Sweby, P.K., 1984. "High resolution schemes using flux limiters few hyperbolic conservation laws". *SIAM Journal on Numerical Analysis*, Vol. 21, pp. 995-1011.

Titarev, V. A. and Toro, E.F., 2004. " Finite-volume WENO schemes for three-dimensional conservation laws". *Journal of Computational Physics*, Vol. 201, pp. 238-260.

Toro, E.F., 1999, *Riemman solvers and numerical methods for fluids dynamics*. Springer, New York, U.S.A.

Zhang, Y.T. and Shu, C. W., 2009. "Third Order WENO scheme on three dimensional tetrahedral meshes". *Communications in Computational Physics*, Vol. 5, pp. 836-848.

Waterson, N. P. and Deconinck H., 2007. "Design principles for bounded higher-order convection schemes - a unified approach". *Journal of Computational Physics*, Vol. 224, pp. 182-207.

7. Responsibility notice

The authors are the only responsible for the printed material included in this paper.